BIOCHEMISTRY
including biophysical chemistry & molecular biology

Article

pubs.acs.org/biochemistry

Vascular Endothelial Growth Factor Peptide Ligands Explored by Competition Assay and Isothermal Titration Calorimetry

Marie Reille-Seroussi,[†] Jean-François Gaucher,[*,‡] Claudia Desole,[†] Nathalie Gagey-Eilstein,[†] Franck Brachet,[‡] Isabelle Broutin,[‡] Michel Vidal,[†,§] and Sylvain Broussy[*,†]

[†]UMR 8638 and [‡]UMR 8015 CNRS, Université Paris Descartes, Faculté de Pharmacie, Sorbonne Paris Cité, 4 av. de l'Observatoire, Paris 75006 France

[§]UF Pharmacocinétique et Pharmacochimie, hôpital Cochin, AP-HP, 27 rue du Faubourg Saint Jacques, Paris 75014, France

Supporting Information

ABSTRACT: The v114* cyclic peptide has been identified as a tight vascular endothelial growth factor (VEGF) ligand. Here we report on the use of isothermal titration calorimetry (ITC), 96-well plate competition assay, and circular dichroism (CD) to explore the binding determinants of a new set of related peptides. Anti-VEGF antibodies are currently used in the clinic for regulating angiogenesis in cancer and age-related macular degeneration treatment. In this context, our aim is to develop smaller molecular entities with high affinity for the growth factor by a structure activity relationship approach. The cyclic disulfide peptide v114* was modified in several ways, including truncation, substitution, and variation of the size and nature of the cycle. The results indicated that truncation or substitution of the four N-terminal amino acids did not cause severe loss in affinity, allowing potential peptide labeling. Increase of the cycle size or substitution of the disulfide bridge with a thioether linkage drastically decreased the affinity, due to an enthalpy penalty. The leucine C-terminal residue positively contributed to affinity. Cysteine N-terminal acetylation induced favorable $\Delta\Delta G°$ and $\Delta\Delta H°$ of binding, which correlated with free peptide CD spectra changes. We also propose a biochemical model to extrapolate K_i from IC_{50} values measured in the displacement assay. These calculated K_i correlate well with the K_d values determined by extensive direct and reverse ITC measurements.

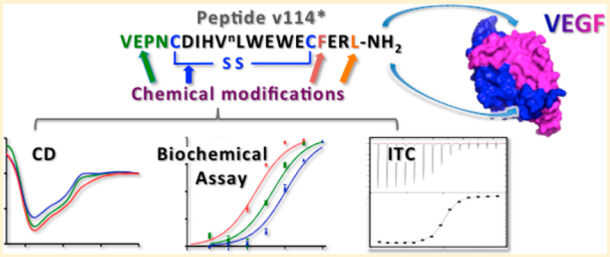

The deregulation of angiogenesis is involved in cancer and inflammatory diseases like atherosclerosis, rheumatoid arthritis, and age-related macular degeneration (AMD).[1,2] The development of molecules able to control angiogenesis is therefore the subject of intense research.[3] In this context, our work is aimed at improving vascular endothelial growth factor A (VEGF) binding peptides. VEGF is the main pro-angiogenic factor, which interacts with several cellular receptors (VEGFR1, -2, and -3) and coreceptors.[4] Among strategies developed to prevent abnormal angiogenesis, disrupting the interaction of the VEGF with its receptors has led to the clinical use of the $VEGF_{165}$ targeting antibodies bevacizumab (Avastin) and ranibizumab (Lucentis) for the treatment of cancer and AMD, respectively.[5] The identification of smaller molecules able to block these protein−protein interactions is also actively pursued, either through binding to the receptor or to the growth factor. Small VEGF-binding proteins, called MiniZ, are currently developed for PET imaging purposes, with K_d values as low as 38 nM, as determined by surface plasmonic resonance (SPR).[6] Disulfide-linked cyclic peptides targeting the VEGF at the receptor binding area have been also identified by phage display (Genentech Inc.)[7] and by bacterial display with a WE/DWE/D consensus sequence.[8] Among them, the peptide v107 (GGNECDIARMWEWECFERL) displaces the VEGF/$VEGFR1_{d2}$ interaction with potency in the low micromolar range by displacement assays.[9] Later, a K_d value of 1 μM has been determined by ITC.[10] The K_d values measured by SPR for v107 and its analogue v114 (VEPNCDIHVMWEWECFERL) are 0.53 and 0.11 μM, respectively.[7] v114* (in which the methionine residue is replaced by a norleucine residue) binds its target with a K_i of 60 nM, as determined by fluorescence polarization displacement assays.[11,12] Alanine scans of v107 and v114 and a "β-scan" of v114* have indicated the position of important amino acids in their peptide sequences.[9,12] These results are consistent with the NMR structure of v107 complex with VEGF, in which amino acids located at the interface show greater sensitivity to alanine mutation.[9]

In order to extend our strategy of disrupting the VEGFR1−VEGF interaction to study the angiogenesis process, we initiated a structure activity relationship (SAR) study on the v114* peptide.[13,14] The following issues were investigated: Could the peptide be shortened without significant loss of affinity through N-terminal and C-terminal deletions? What are the effects induced by variations of the macrocycle size and the nature of the covalent bond? What is the effect of incorporation of non-proteinogenic amino acids? Moreover, to screen the current and future synthesized analogues by a high throughput

Received: June 27, 2015
Published: July 29, 2015

DOI: 10.1021/acs.biochem.5b00722
Biochemistry 2015, 54, 5147−5156

method, we evaluated the use of a displacement assay (coated $VEGFR1_{ECD}$/*bt*$VEGF_{165}$) for IC_{50} determination.[15] These results were compared to the K_d values and to the thermodynamic parameters measured by extensive direct and reverse isothermal titration calorimetry (ITC) measurements. Then a biochemical model of binding was proposed to extrapolate K_i from IC_{50}. This approach has yielded shortened molecules with a small loss of affinity for the target and rationalized the design of new peptides.

EXPERIMENTAL PROCEDURES

Peptides Synthesis and Characterization (HPLC, Mass Spectrometry, CD). N^{α}-Fmoc amino acids with standard side chain protections and coupling reagents (DIC, HOBt, OxymaPure and DIEA) were purchased from SDS Carlo-Erba. The NovaSyn TGR resin (loading 0.25 mmol/g) was obtained from Novabiochem. All other reagents were purchased from Aldrich. All solvents were purchased from SDS Carlo-Erba.

HPLC analysis was performed on a Phenomenex Luna C18 column (5 μm, 4.6 × 250 mm), with the following solvents system: solvent A was water with 0.1% TFA, and solvent B was a 70% acetonitrile in water solution with 0.09% TFA. Peptides were purified by semipreparative HPLC on a Grace Alltima C18 column (5 μm, 10 × 250 mm) using a gradient program from 20 to 100% B in 60 to 100 min, at a flow rate of 2 mL/min. Products were detected by UV at 220 and 254 nm.

For mass spectrometry analysis, MALDI spectra were recorded on an Applied Biosystems 4700 proteomic analyzer spectrometer at UPMC (Paris, France) (Figure S1, Table S1, Supporting Information).

Circular dichroism (CD) experiments were performed on a Jobin-Yvon model C8 spectropolarimeter calibrated with (1*S*)-(+)-10-camphorsulfonic acid. Spectra were recorded at 18 °C in a 0.1 cm cell between 190 and 260 nm with a bandwidth of 2.0 nm, a response time of 2 s, and a resolution step width of 0.5 nm. Each spectrum represents the average of five scans. Lyophilized peptide samples were weighed and dissolved in 18.2 MΩ distilled water to prepare stock solutions at about 500 μM. Each stock solution was then diluted five times in phosphate buffer 10 mM pH 7.4 to obtain a final concentration of about 100 μM. The accurate final concentrations were determined by UV with molar extinction coefficients calculated using literature data ($\varepsilon_{280\ nm}$ = 11 225 $L{\cdot}mol^{-1}{\cdot}cm^{-1}$).[16]

Peptides were synthesized on solid phase and under microwave irradiation on a 0.1 mmol scale with NovaSyn TGR resin using a CEM Liberty 1 synthesizer. Microwave irradiation was employed following the synthesizer provider recommendations for both coupling and deprotection steps. Coupling reactions were performed using N^{α}-Fmoc amino acids (5 equiv related to the resin) activated with DIC (4.9 equiv) and OxymaPure (10 equiv). After each coupling step, Fmoc removal was effected by treating the resin with 20% piperidine in DMF. When required, the peptides were acetylated using a mixture of acetic anhydride (0.5 M) and DIEA (0.125 M) in DMF (10 mL). The reaction was stirred at room temperature for 15 min and washed with DMF. Alternatively, the desired carboxylic acid was coupled manually to the resin. The coupling reaction was performed in DMF using the suitable acid (10 equiv related to the resin) activated with DIC (10 equiv) and HOBt (10 equiv). The reaction was monitored by chloranil analysis. After completion, the resin was washed with DMF and dichloromethane. The deprotection and cleavage of the peptides from the resin were performed by treatment with 10 mL of TFA/H_2O/EDT/TIPS (94:2.5:2.5:1.0) for 3 h at room temperature (except for the linear peptide **15** which was cleaved without EDT). After removal of the resin, the filtrate was concentrated under a stream of argon and precipitated with cold diethyl ether. The precipitate was isolated by centrifugation and washed with diethyl ether, affording the crude peptides. With the exception of the linear peptide **15**, cyclization was carried out at 1 mM peptide concentration by addition of a 100 mM solution of $NH_4{\cdot}HCO_3$. Disulfide formation was monitored by HPLC and Ellman analysis.[17,18] After completion of the reaction, the solvent was evaporated, and the crude peptides were purified by semipreparative HPLC. The products were collected and analyzed by HPLC. Pure fractions were pooled and lyophilized to yield the peptides as white solids. Yields were comprised between 5 and 20% for all peptides.

The thioether peptide **14** was synthesized from the purified peptide **11** (20 mg), dissolved in 50 mL of a solution of water/triethylamine (9:1). The reaction was stirred at room temperature and monitored by HPLC and Ellman analysis until complete conversion (7 days). Then, the triethylamine was evaporated under a vacuum, and the peptide was lyophilized. The crude peptide was purified by semipreparative HPLC using a gradient 20−100% B in 60 min (with a gentle slope between 65 and 75% of B). The product was collected and analyzed by HPLC (Figure S1, Table S1, Supporting Information). Pure fractions were pooled and lyophilized to obtain the desired thioether peptide **14** as a white solid in 19% yield (1:1 mixture of diastereomers).

VEGF Expression and Purification. The VEGF expression and purification method was derived from previously reported procedures.[19] A synthetic gene encoding the human VEGF protein (residues 13−107) was cloned into pET22b(+) expression vector (Novagen, Merck, Darmstadt, Germany) and introduced into the *Escherichia coli* Rosetta 2 bacterial strain (Novagen, Darmstadt, Germany). Cultures were grown at 37 °C in LB supplemented with 150 μg/mL ampicillin, and protein expression was induced by 0.5 mM isopropyl β-D-1-thiogalactopyranoside. VEGF was expressed as an insoluble protein. Cells were lysed by ultrasonic disruption in Tris/Hepes buffer (50 mM/50 mM pH 8.1) containing 1% (w/v) Triton X-100. Inclusion bodies were isolated by centrifugation at 9500*g* 20 min. The pellet was further purified by three successive steps of sonication, washing (50 mM/50 mM Tris/Hepes pH 8.0, 1 M NaCl), and 40000*g* centrifugations. Typically 160 mg of protein was solubilized in 125 mL of buffer containing 8 M urea, 4 mM DTT, 12.5 mM Tris/HCl pH 8.1, 250 mM NaCl, and 5 mM imidazole and dialyzed overnight in 20 volumes of 50 mM Na_3 citrate, 1 mM cysteine at 4 °C. Then it was dialyzed successively in 20 volumes of 20 mM Tris/HCl pH 8.1, 1 mM $CuSO_4$, and 20 volumes of 20 mM Tris/HCl pH 8.1, 250 mM NaCl. Misfolded proteins were discarded by 20 min 40000*g* centrifugation, and then the supernatant was dialyzed two times against 20 mM Tris/HCl pH 8.1. Refolded homodimeric protein was purified by anion-exchange chromatography on a Source 15Q column (Amersham-GE Healthcare, Little Chalfont, UK) in 20 mM Tris/HCl pH 8.1 and eluted with a 1 M NaCl gradient in the same buffer. The main elution peak corresponded to refolded VEGF. Purity and homogeneity of disulfide bonding were checked on SDS-PAGE, with and without thiol reduction. The protein was eluted as a unique peak of 20.3 kDa apparent mass on analytical size exclusion chromatography (SEC) (Superdex 75 HR 10/30 Amersham-

DOI: 10.1021/acs.biochem.5b00722
Biochemistry 2015, 54, 5147−5156

GE Healthcare, Little Chalfont, UK). The VEGF concentration was measured by UV absorption at 280 nm with a molecular mass of 22 230 Da and $\varepsilon_{280\ nm}$ = 12 920 L·mol^{-1}·cm^{-1}. Protein was dialyzed three times in pure water, concentrated by ultrafiltration, lyophilized, and stored at −80 °C.

Displacement Assay. In the present study, IC_{50} and K_i values were determined by displacement of *bt*VEGF$_{165}$ from coated VEGFR1$_{ECD}$. The purified proteins (*bt*VEGF$_{165}$ and VEGFR1$_{ECD}$) were purchased from R&D. SuperSignal West Pico Substrate (HRP substrate) was purchased from Pierce. Bovine serum albumin fraction IV (BSA) and Tween 20 were obtained from Sigma-Aldrich and AMDEX streptavidin-horseradish peroxidase from Amersham Biosciences. White high-binding 96-well plates were purchased from Costar.

Displacement assays were performed as previously described with small modifications of the procedure.[15] Briefly, a white high-binding 96-well plate was coated overnight at 4 °C with the VEGFR1$_{ECD}$ (20 ng in 100 μL of PBS per well). The plate was washed 3 times with PBS containing 0.1% Tween 20 (v/v, buffer A) and 200 μL of 3% BSA in PBS (w/v) were added. After 2 h at 37 °C, the plate was washed 3 times with buffer A, and the peptides were added at 2× concentration in 50 μL of PBS with 2% DMSO. A total of 50 μL of a solution of *bt*VEGF$_{165}$ (20 pM in PBS, nominal concentration) was added to each well, and the resulting solutions were mixed with 4 micropipette actions. After 2 h incubation at 37 °C, the plate was washed 4 times with buffer A. A total of 100 μL of AMDEX streptavidine-horseradish peroxidase diluted at 1:8000 in PBS containing 0.5% (v/v) Tween 20 and 0.3% (w/v) BSA was added to each well. After 45 min incubation at 37 °C in the dark, the plate was washed five times with buffer A and 100 μL of SuperSignal West Pico Substrate was added. The plate chemiluminescence (as relative lights units, RLU) was rapidly read on a PerkinElmer Victor 2 spectrophotometer. The percentages of displacement were calculated using the formula: % displacement = 100[1 − (S − NS)/(MS − NS)], where S is the measured signal, and NS and MS are nonspecific (no VEGFR1$_{ECD}$ coated) and maximum (no inhibitor) signals, respectively. Data were analyzed with the software Graphpad Prism using a "log [inhibitor] vs. response" nonlinear regression.

ITC Assay. ITC assays were performed on a Microcal TM ITC200 system at 20 °C. Both components were dissolved in the same assay buffer: 50 mM Hepes/NaOH, pH 7.5, 150 mM NaCl, 1% (v/v) DMSO. Ligands and protein concentrations were determined by UV absorption at 280 nm from three independent dilutions of stock solutions in assay buffer. Typical measurements were carried out by 18 × 2.14 μL to 40 × 0.96 μL successive microinjections of solutions of titrant into the reactor containing the titrated molecule (initial injection of 0.4 μL), with a 120−180-s spacing time between injections, stirring of 1000 rpm, and a reference power of 5 μcal/s. With the exception of peptides **3** and **12**, we measured both direct and reverse titration, i.e., the titration of VEGF by peptide solution and the titration of peptides solution by VEGF solution (concentrations indicated in the Supporting Information, Table S2). Injection parameters (volume, number of measures, and spacing time) and concentrations of ligands and VEGF were adjusted depending on peptide affinities and heat of binding, to obtain a better accuracy for the determination of the thermodynamic parameters. The key parameter $c = K_a[M_0]n$, where $[M_0]$ is the titrated molecule concentration and n the stoichiometry parameter, was in the range from 5 to 500 for most of the assays.

The ITC data were initially analyzed by the software ORIGIN with a nonlinear, one set of site model. In a second step, the data were integrated and the standard deviations were estimated by the software NITPIC and then analyzed by SEDPHAT (https://sedfitsedphat.nibib.nih.gov/software/default.aspx) with a global modeling of titration isotherm for each peptide. Graphical representations of results were from GUSSI.[20,21] The binding thermograms were analyzed with the two identical sites binding model of SEDPHAT.[22] In this software, the binding of an inhibitor I to a VEGF macromolecule V at two identical sites and in the absence of cooperativity effect is characterized by the unique microscopic constant k for a single site:

$$k = \frac{VI}{V \times I} = \frac{IV}{V \times I} = \frac{VI_2}{VI \times I} = \frac{VI_2}{IV \times I}$$

The macroscopic association constant for the first binding K_1 was given by

$$\frac{1}{K_d} = K_1 = \frac{(VI)_\Sigma}{V \times I} = \frac{IV + VI}{V \times I} = 2k \quad (1)$$

Similarly the binding macroscopic binding constants to the second site K_2 and K_{VI_2} were expressed as

$$K_2 = \frac{VI_2}{(VI)_\Sigma \times I} = \frac{VI_2}{(VI + IV) \times I} \quad (2)$$

$$\Rightarrow K_2 = \frac{k}{2} = \frac{K_1}{4} \quad (3)$$

and

$$K_{VI_2} = \frac{VI_2}{V \times I^2} = K_1 \times K_2 = k^2$$

RESULTS

Peptide Synthesis. All peptides (Table 1) were synthesized by the Fmoc method on an automatic solid phase synthesizer with the recently developed DIC/OxymaPure system, because it is safer than benzotriazole-based systems.[23] After cleavage from the resin and deprotection of the side chains, the disulfide cyclization was achieved by air oxidation in a diluted basic aqueous solution. Most peptides were completely cyclized within a few hours up to a day (Figure S2, Supporting Information). However, striking differences in the cyclization kinetics were observed among the *N*-terminal modified peptides. For example, the reaction was almost complete in less than 1 h for peptide **6** but required several days for peptide **3**. In the case of **6**, the strong rate acceleration might be explained by the presence of a stacking interaction between the naphthyl group (resembling a tryptophan side chain) and one of the tryptophan residues, inducing a favorable preorganization. This hypothesis would have to be confirmed by additional experimental or computational work but is supported by previous observations with tryptophan containing peptides.[24,25]

In addition to these peptides cyclized via a disulfide bridge, we synthesized an analogue cyclized by a thioether bond. We initially envisioned a synthetic strategy allowing the production of the desired thioether peptide as a single diastereomer, mediated by an intramolecular cyclization of the Cys 15 thiol

DOI: 10.1021/acs.biochem.5b00722
Biochemistry 2015, 54, 5147−5156

Table 1. Sequences of v114* Analogues[b]

Peptide	Sequence (1 5 10 15)
v114*	VEPNCDIHV^{n}LWEWECFERL-NH_2
1	CDIHV^{n}LWEWECFERL-NH_2
2	deamino-CDIHV^{n}LWEWECFERL-NH_2
3	Ac-CDIHV^{n}LWEWECFERL-NH_2
4	4-pentynoyl-CDIHV^{n}LWEWECFERL-NH_2
5	phenylacetyl-CDIHV^{n}LWEWECFERL-NH_2
6	2-naphtylacetyl-CDIHV^{n}LWEWECFERL-NH_2
7	CDIHV^{n}LWEWECFER-NH_2
8	CDIHV^{n}LWEWE^{h}CFER-NH_2
9	^{h}CDIHV^{n}LWEWE^{h}CFER-NH_2
10	Ac-CDIHV^{n}LWEWECFER-NH_2
11	Ac-CDIHV^{n}LWEWE^{h}CFER-NH_2
12	Ac-^{h}CDIHV^{n}LWEWE^{h}CFER-NH_2
13	deamino-CDIHV^{n}LWEWE^{h}CFER-NH_2
14[a]	Ac-dethio-CDIHV^{n}LWEWE^{h}CFER-NH_2
15	SDIHV^{n}LWEWESFERL-NH_2
16	CDIHV^{n}LWEWEC^{n}FER-NH_2
17	CDIHV^{n}LWEWEC^{F}FER-NH_2

[a]Mixture of diastereomers. [b]Amino acids are numbered in reference to v114*. ^{n}L denotes norleucine, ^{h}C homocysteine, ^{F}F *para*-fluoro-phenylalanine and ^{n}F *para*-nitro-phenylalanine residues.

functional group onto an electrophilic carbon. However, the introduction of the required halogenated function at the N-terminal position proved problematic. In accordance with reports in the literature, we observed a very low coupling efficiency of the halogenated derivative on the peptide.[26,27] In this context, an alternative desulfurization strategy under basic conditions was employed.[28−30] Cys 15 was replaced by a homocysteine residue to decrease the number of diastereomers potentially produced during the course of the reaction. This precaution has the additional advantage of leading to a cystathionine-type covalent link, instead of a lanthionine-type. Consequently, the peptide **14** containing the same number of atoms as the peptide **10** within the macrocycle (35 atoms) was obtained as a mixture of only two diastereomers.

Isothermal Calorimetry. ITC measurements were obtained for selected compounds to determine thermodynamic parameters of binding, i.e., equilibrium constant K_a, the enthalpy change $\Delta H°$, and the stoichiometry parameter n.

Concentrations were determined by absorption measurements of triplicate dilutions of solutions with relative error of reproducibility lower than 5%. Under these experimental conditions, we observed that the titration of peptides by VEGF resulted in a protein/peptide mean stoichiometry of 1:1.93 (Std = 0.16, 32 independent titrations analyzed with ORIGIN). The reverse titration of VEGF by peptides resulted in an unexpected mean stoichiometry of 1:1.52 (Std = 0.16, 21 independent titrations), which may reflect an underestimation of the concentration of the peptide solutions. However, the VEGF is a homodimeric protein displaying two symmetrical binding sites for peptides, and a binding stoichiometry of 1:2 is accepted. Consequently we fixed the VEGF/ligand stoichiometry and used the "two-symmetrical site" SEDPHAT model of binding. Scale correction factors to concentrations of titrated and titrating molecules were refined in each experiment, and the discrepancy with apparent stoichiometry was corrected as an underestimation of peptide concentration, when used as titrant, by SEDPHAT software.[20] The direct and reverse titrations for each peptide were combined, and the thermodynamic parameters were calculated by the global modeling of titration isotherms. This method is a particularly efficient way to evaluate potential cooperativity effects. However, the thermograms displayed obvious one phase patterns, in both direct and reverse titration, and no binding cooperativity was suspected, which was confirmed by fitting attempts.

All of the global SEDPHAT analysis converged to robust parameters, with the exception of peptides **9** and **12**, which reached the technical limitation of ITC measurement because of their low affinity (K_d = 20 μM). Moreover, peptide **12** was not used for the direct titration of the protein, and peptide **3** for the reverse titration. This results in the thermodynamic parameters of these peptides being less reliable, especially enthalpy and entropy values.

The error analysis (P = 0.95) carried out with the automatic confidence procedure of SEDPHAT gave realistic confidence, which is greatly improved as compared with single assay analysis by ORIGIN software. Characteristic thermograms for peptides are given in Figure 1 and in Figure S3, Supporting Information. Refined parameters are described in Supporting Information, Table S2, and summarized in Table 2 and Figure 2.

Comparison of Competition Assay and ITC. We observed an obvious correlation between the IC_{50} and K_d values, with the exception of peptide **12**, which was a striking outsider and was left out of the study. This correlation indicated that the displacement assay was useful for a semiempirical approach of affinity ranking of the compounds (Figure 3). However, we had to reconsider the analytical approach of binding. Indeed this assay was initially developed to screen receptor ligands. Therefore, the classical Cheng−Prusoff equation was usable to calculate the K_i of ligands in competition with *bt*VEGF for the receptor $VEGFR1_{ECD}$.[31] This entails $K_i = IC_{50}/(1 + V_0/K_d')$, where V_0 was the *bt*VEGF concentration, and K_d' was the dissociation constant of *bt*VEGF for the receptor (K_d' = 750 pM).[15]

In the present case, the assay was used in an unusual setup, where the peptides competed with the fixed receptor for the *bt*VEGF in solution. Moreover *bt*VEGF has two equivalent binding sites for peptide. Consequently the following scheme may be proposed for competitive inhibitors:

$$VI_2 + R \overset{K_2}{\rightleftarrows} (VI)_\Sigma + I + R \overset{K_1}{\rightleftarrows} V + 2I + R \overset{K'}{\rightleftarrows} VR + 2I$$

The macroscopic association constants are

$$K_1 = \frac{(VI)_\Sigma}{V \times I} \quad (1)$$

DOI: 10.1021/acs.biochem.5b00722
Biochemistry 2015, 54, 5147−5156

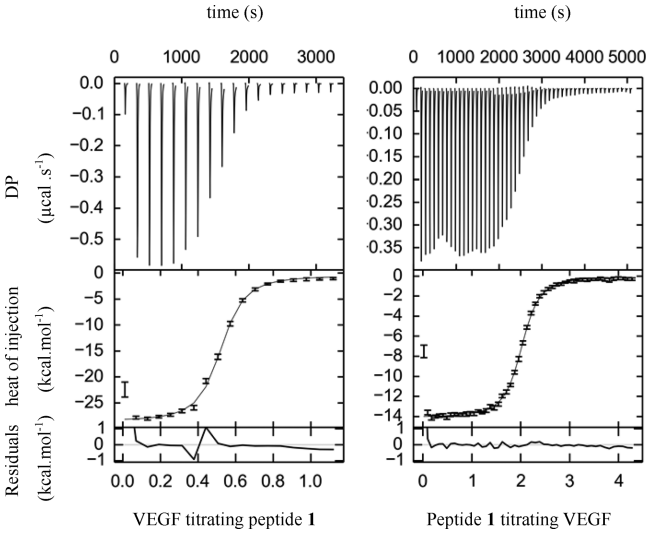

Figure 1. Representative isothermal titrations of peptides with VEGF and of VEGF with peptides. The upper panel for each figure represents ITC thermograms, while the bottom panel represents the integrated areas under each peak, standard deviations, and best fit curves. Note that $n = 0.5$ for the direct titration of VEGF by peptide and $n = 2$ for the reverse titration reflect the 1:2 stoichiometry of the interaction. First injections are discarded from curve fitting.

$$K_2 = \frac{VI_2}{(VI)_\Sigma \times I} \tag{2}$$

$$K' = \frac{VR}{V \times R} \tag{4}$$

I and R are the free peptide and free receptor molar concentrations, respectively.

The total *bt*VEGF concentration is

$$V_0 = V + VR + (VI)_\Sigma + VI_2$$

With eq 1 and eq 2

$$V_0 = VR + V \times (1 + K_1 \times I \times (1 + K_2 \times I))$$

The ITC data proved that the two binding sites were undistinguishable, and no cooperativity occurred upon peptide binding to VEGF. Consequently and for statistical reasons, as previously explained in eq 3

$$K_2 = \frac{K_1}{4}, \text{ and } V_0 = VR + V \times \beta \text{ with } \beta = 1 + K_1 \times I \times \left(1 + \frac{K_1}{4} \times I\right) \tag{5}$$

Moreover since $V_0 \ll R_0$, then $R_0 = R + VR \approx R$

From eqs 4 and 5, we have

$$\frac{VR}{K'} = (V_0 - VR) \times \frac{R_0}{\beta} \Rightarrow VR = \frac{V_0 \times \frac{R_0}{\beta}}{\frac{1}{K'} + \frac{R_0}{\beta}} \tag{6}$$

The assay quantifies the *bt*VEGF bound to the receptor; i.e., the signal is proportional to VR.

The relative signal is

$$\frac{\phi}{\phi_{max}} = \frac{VR}{VR_{max}} = \frac{V_0 \times \frac{R_0}{\beta}}{\frac{1}{K'} + \frac{R_0}{\beta}} \times \frac{\frac{1}{K'} + R_0}{V_0 \times R_0} = \frac{\frac{1}{K'} + R_0}{\frac{\beta}{K'} + R_0} \tag{7}$$

When $I_0 = IC_{50}$, then $(\phi/\phi_{max}) = (1/2)$ and eq 7 = > $\beta = 2 + K' \times R_0$

Combined with 5, we obtain

$$K_1^2 + K_1 \times \frac{4}{I} - \frac{4}{I^2} \times (1 + K' \times R_0) = 0$$

The equation results in a single positive root:

$$K_1 = \frac{2}{I} \times (\sqrt{2 + K' \times R_0} - 1) \tag{8}$$

In the assay conditions, we hypothesized that some nonspecific adsorption of peptide may occur, reflected by the term ε. Then, $IC_{50} = I + (VI)_\Sigma + 2 \times VI_2 + \varepsilon$.

The depletion effect is negligible, indeed, $V_0 \ll IC_{50} \Rightarrow (VI)_\Sigma + 2 \times VI_2 \ll IC_{50}$, and therefore $IC_{50} \approx I + \varepsilon$, and with 8

$$K_i = \frac{1}{K_1} = a \times IC_{50} + b \tag{9}$$

where

Table 2. Thermodynamic Parameters of v114* Analogues Binding on VEGF, Determined by ITC[a] at 20 °C

peptide	$\Delta G°$ (kcal·mol^{-1})	$\Delta H°$ (kcal·mol^{-1})	$-T\Delta S°$ (kcal·mol^{-1})	nd:nr[b]
v114*	−10.1 [−10.0; −10.3]	−16.6 [−16.3; −16.8]	6.4 [6.0; 6.8]	4:2
1	−9.2 [−9.0; −9.4]	−14.1 [−13.6; −14.6]	4.9 [4.2; 5.5]	4:2
2	−9.3 [−9.1; −9.5]	−15.4 [−15.1; −15.9]	6.1 [5.6; 6.7]	2:2
3	−9.7 [−9.5; −9.8]	−15.2 [−14.8; −15.6]	5.5 [5.1; 6.0]	0:2
4	−9.2 [−9.0; −9.3]	−15.2 [−14.9; −15.5]	6.0 [5.6; 6.4]	2:2
5	−9.5 [−9.3; −9.6]	−15.7 [−15.4; −16.0]	6.2 [5.8; 6.7]	2:2
7	−8.2 [−8.1; −8.3]	−14.7 [−14.5; −15.1]	6.5 [6.2; 7.0]	2:2
8	−7.5 [−7.4; −7.6]	−13.2 [−12.8; −13.5]	5.7 [5.3; 6.1]	2:1
9	−6.3 [−6.1; −6.6]	−12.6 [−11.3; −14.7]	6.3 [4.8; 8.6]	1:1
10	−8.8 [−8.7; −8.9]	−16.6 [−16.3; −16.8]	7.8 [7.5; 8.1]	2:1
11	−7.6 [−7.5; −7.7]	−15.5 [−15.1; −15.9]	8.0 [7.5; 8.3]	2:1
12	−6.3 [−6.2; −6.5]	−13.7 [−12.7; −14.9]	7.4 [6.3; 8.7]	2:0
14	−7.5 [−7.4; −7.7]	−15.7 [−15.2; −16.2]	8.1 [7.6; 8.7]	2:1
17	−7.1 [−7.0; −7.2]	−11.0 [−10.7; −11.3]	3.9 [3.6; 4.2]	2:2

[a]95% confidence intervals are given in brackets. Parameters are normalized for one binding site. Peptides **6**, **13**, **15**, and **16** were not analyzed by ITC because they were unavailable or insoluble. [b]"nd:nr" refers to the number of direct and reverse titrations of VEGF by peptide used for the global analysis of ITC assay.

DOI: 10.1021/acs.biochem.5b00722
Biochemistry 2015, 54, 5147−5156

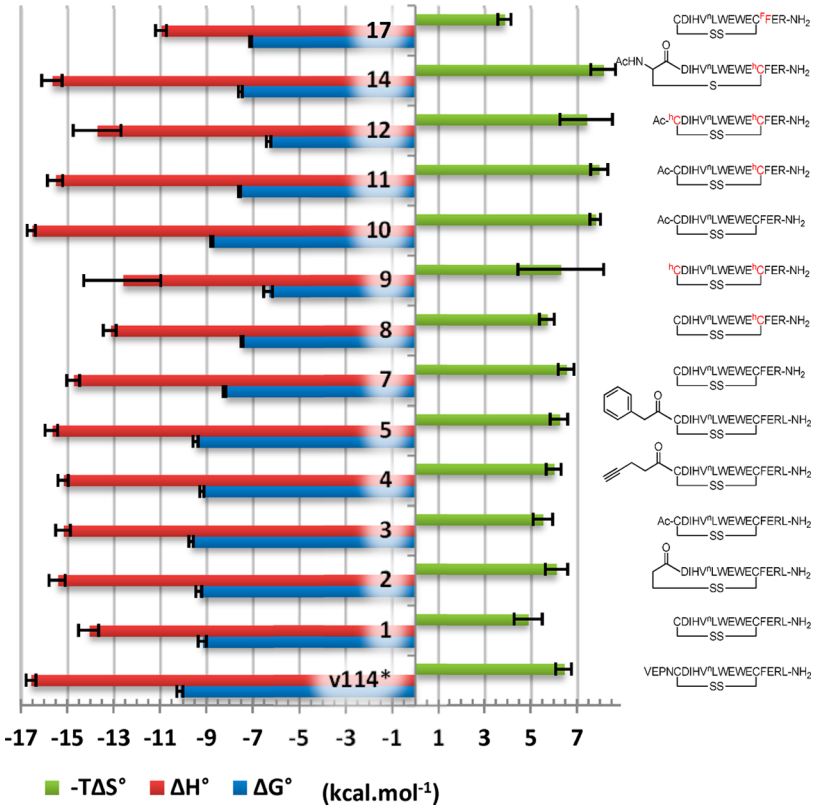

Figure 2. Overview summarizing thermodynamic parameters of peptide–VEGF interactions (kcal·mol^{-1} of binding site).

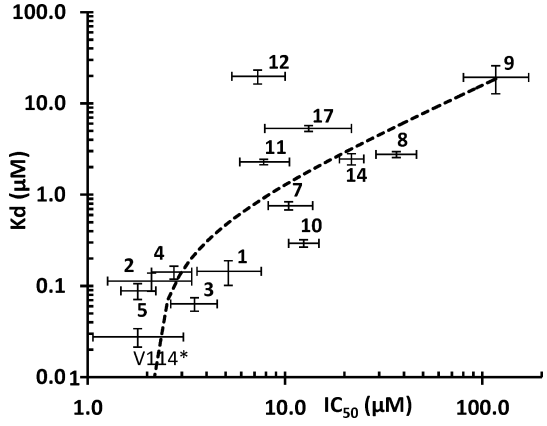

Figure 3. Comparison between IC_{50} values obtained from the $VEGFR1_{ECD}$/*bt*$VEGF_{165}$ displacement assay) and K_d values from ITC measurements. Error bars represent 95% confidence intervals. Dashed line is the linear regression fit $K_d = 0.16 \times IC_{50} - 0.34$ (μM) ($R^2 = 0.92$). Peptide **12** was excluded from regression fit.

$$a = \frac{1}{2(\sqrt{2 + K' \times R_0} - 1)}, \text{ and } b = -a \times \varepsilon$$

Estimation of "a" may be calculated with R_0 set to the upper limit of receptor concentration coated on the plate, considering a full binding. In our conditions, $R_0 = 1$ nM and $K' = 1.33 \times 10^9$ M^{-1}.[15] It leads to $K_i = 0.61 \times (IC_{50} - \varepsilon)$ (μM).

Experimentally, when minimizing the linear relation between K_d and IC_{50}, the following empirical relation was obtained $K_i = 0.16 \times IC_{50} - 0.34$ (μM) eq 9, with $R^2 = 0.92$.

Nonspecific binding is then estimated to $\varepsilon = -(b/a) = 2.1$ μM.

Effects of N-Terminal and C-Terminal Truncations. The removal of the four N-terminal residues of the parent peptide v114* (leading to peptide **1**, Table 1) resulted in loss of affinity for VEGF across the two biochemical assays: the displacement assay (3-fold increase in the IC_{50} value) and the ITC measurements (6-fold increase in the K_d value) (Table 3). In an attempt to regain the affinity lost by truncation, the four amino acids were replaced by different hydrocarbon substituents (peptides **3**–**6**, Table 1). No significant differences in IC_{50} values or between binding affinities and thermodynamic parameters were observed for **1**, **4**, and **5** among this subset of peptides. Similarly, *N*-terminal deamination (peptide **2**) had only a slight effect. Interestingly, acetylation resulted in over a 2-fold decrease in the K_d value for peptide **3** (64 nM) as compared to peptide **1** (145 nM).

Deletion of the C-terminal Leu 19 residue in peptide **1** to give peptide **7** resulted in a 2-fold increase in IC_{50} in the $VEGFR1_{ECD}$/*bt*$VEGF_{165}$ displacement assay (Table 3), but ITC measurements indicated a 5-fold lower affinity ($\Delta\Delta G° = 1.0 \pm 0.3$ kcal·mol^{-1}, Table 2). Deletion of the Leu 19 residue in acetylated peptide **3** to give peptide **10** induced a similar loss of binding affinity ($\Delta\Delta G° = 0.9 \pm 0.2$ kcal·mol^{-1}). For both peptides **7** and **10**, Leu 19 deletion induced an entropy penalty ($\Delta(-T\Delta S°) = 1.6 \pm 1.0$ and 2.3 ± 0.8 kcal·mol^{-1} respectively). Small differences were observed in CD spectra of compounds v114*, **1** and **7**. In particular, peptide **7**, lacking the C-terminal leucine capping the α-helical segment, appeared slightly less structured (Figure 4).

For these first series of modified peptides **1**–**7** and **10**, truncations and replacements resulted in rather small changes in binding parameters $\Delta\Delta H°$ and $\Delta(-T\Delta S°)$. At most, $\Delta\Delta H°$ values of 2.5 kcal·mol^{-1} were observed between v114* and

DOI: 10.1021/acs.biochem.5b00722
Biochemistry 2015, 54, 5147–5156

Table 3. Outcome of Competition Assay and ITC

peptide	IC_{50} ECD (μM)[a]	K_i (μM)[b]	K_d (μM)[c]
v114*	1.8 [1.1; 3.0]	NV [0.0; 0.2]	0.028 [0.022; 0.035]
1	5.2 [3.6; 7.5]	0.5 [0.2; 0.9]	0.145 [0.101; 0.189]
2	2.1 [1.3; 3.3]	NV [0.0; 0.2]	0.113 [0.089; 0.141]
3	3.5 [2.7; 4.5]	0.2 [0.08; 0.4]	0.064 [0.053; 0.076]
4	2.7 [2.2; 3.4]	0.1 [0.0; 0.2]	0.142 [0.121; 0.168]
5	1.8 [1.5; 2.2]	NV [0.0; 0.1]	0.089 [0.072; 0.107]
6	5.7 [4.3; 7.5]	0.6 [0.3; 0.9]	not determined
7	10.4 [8.3; 13.7]	1.3 [0.9; 1.9]	0.761 [0.694; 0.850]
8	36.6 [28.9; 46.3]	5.5 [4.2; 7.1]	2.76 [2.53; 2.96]
9	117 [80; 171]	18 [12; 28]	19.3 [14.1; 27.3]
10	12.4 [10.5; 14.8]	1.7 [1.3; 2.1]	0.294 [0.271; 0.325]
11	7.8 [5.9; 10.5]	0.9 [0.6; 1.4]	2.28 [2.10; 2.42]
12	7.3 [5.4; 10.0]	0.8 [0.5; 1.3]	19.8 [16.7; 23.7]
13	9.2 [8.4; 10.1]	1.1 [1.0; 1.3]	not determined
14	21.7 [18.9; 25.0]	3.1 [2.7; 3.7]	2.46 [2.13; 2.83]
15	>100[d]	>15	not determined
16	23.8 [15.6; 36.1]	3.5 [2.1; 5.5]	not determined
17	13.2 [8.0; 21.7]	1.8 [0.9; 3.2]	5.31 [4.94; 5.74]

[a]"IC_{50} ECD" refers to the IC_{50} values obtained in the $VEGFR1_{ECD}$/*bt*$VEGF_{165}$ displacement assay. 95% confidence intervals are given in brackets. [b]K_i values determined from IC_{50} values according to the equation $K_i = 0.16 \times IC_{50} - 0.34$ (μM) (see Results). 95% confidence intervals are given in brackets (errors estimation expended only from IC_{50} errors). NV refers to negative values calculated from $IC_{50} < 2.1$ μM, which are without physical significance (see Discussion). [c]K_d values determined by ITC assay. 95% confidence intervals are given in brackets. [d]Peptide **15** was insoluble at concentrations >100 μM.

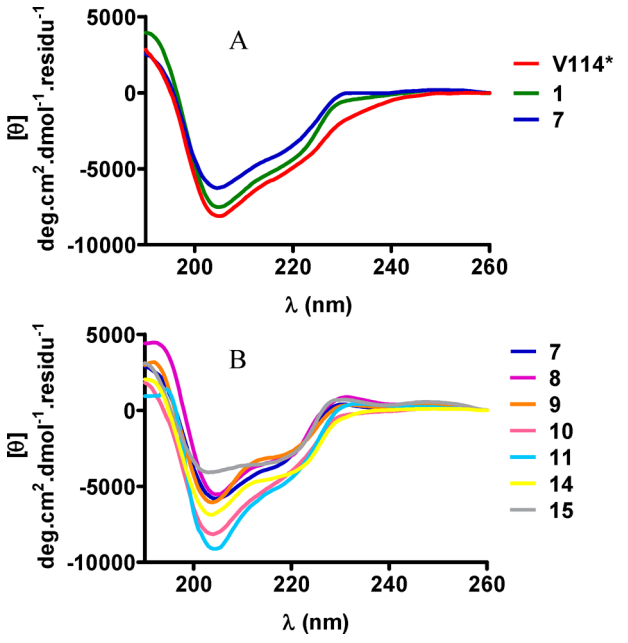

Figure 4. Circular dichroism spectra of (A) peptides v114* (red), **1** (green), and **7** (blue), showing the effect of sequence shortening; (B) peptides **7** (blue), **8** (purple), **9** (orange), **10** (pink), **11** (aqua), **14** (yellow), **15** (gray), showing the effect of modifications of the nature and size of cyclization. Spectra were recorded in 10 mM sodium phosphate buffer (pH 7.4, 18 °C). See Experimental Procedures for details.

peptide **1** and 1.9 kcal·mol^{-1} between v114* and peptide **7**, accounting for the 27 fold increase in K_d.

Effects of the Variations of the Cycle Size and Nature. The influence of the disulfide bridge on the peptide conformation and affinity for VEGF was explored by circular dichroism and biochemical assays. A control linear peptide **15** was synthesized, in which both cysteine residues were substituted by serine residues to prevent unwanted spontaneous cyclization. As expected, it did not show any activity up to 100 μM in the displacement assay (Figure S4B, Supporting Information). CD measurements indicated a decrease in the degree of secondary structure of the linear peptide compared to disulfide-bridged peptides (Figure 4), which explains its lack of binding efficiency.

Then, the effect of a variation of the cycle size on VEGF binding was probed by successively replacing one (Cys 15) or both cysteine residues with homocysteine residues. This was accomplished for a series of nonacetylated peptide (**7**, **8**, **9**) and reproduced in a series of acetylated peptide (**10**, **11**, **12**). Within each series, increasing the macrocycle size by one or two carbon atoms resulted in a decrease in affinity (25-fold K_d increase from **7** to **9**, and 70-fold from **10** to **12**). This result was reproducible among the two series and was predominantly the consequence of an unfavorable binding enthalpy change (about 1.2 kcal·mol^{-1} for each homocysteine residue added).

Replacement of the sulfur atom of Cys 15 in peptide **10** by a carbon atom in peptide **14**, thereby replacing the disulfide bridge by a thioether bridge, resulted in a decrease in affinity (Table 3, K_d) and a loss of α-helical structure as suggested by CD (Figure 4B). The estimated 2-fold loss of IC_{50} by displacement assay corresponded to an 8-fold decrease of the K_d value, apparently due to an enthalpy penalty (Table 2).

Effect of Acetylation at the N-Terminal End. The comparison between the nonacetylated (**1**, **7**, and **8**, and **9**) and acetylated (**3**, **10**, **11**, and **12**) series indicated, in all four cases, different thermodynamics of binding (Table 2). Indeed, when peptides **1**, **7**, and **8**, are compared to **3**, **10**, and **11**, respectively, acetylation induced a systematic increase in affinity ($\Delta\Delta G^\circ$ = −0.4 kcal·mol^{-1} on average), and a consistently favorable enthalpy variation, corresponding to $\Delta\Delta H^\circ$ from −1.1 to −2.4 kcal·mol^{-1}. However, the entropy of binding became more unfavorable with increasing $T\Delta S^\circ$. We noticed that the overall trends of peptides **9** and **12** are similar, although not significant given the uncertainty of their thermodynamic parameters.

Visible differences in the CD spectra of the acetylated and nonacetylated peptides (Figure 4) showed that the $\Delta\Delta H^\circ$ and $\Delta(-T\Delta S^\circ)$ may arise from a distinct preorganization of the free peptides.

Effect of the Modification of the Phe 16 Residue. The introduction of a nitro group at the *para* position of Phe 16 induced a 2-fold decrease in displacement potency (IC_{50} and K_i extrapolated from IC_{50} of peptide **16** compared to peptide **7** in Table 3). Interestingly, the introduction of a fluorine atom at the same position did not significantly change the IC_{50} value in the displacement assay (peptide **17**). But, when evaluated in the ITC assay, a 7-fold loss in affinity was measured for peptide **17** as compared to **7** (ΔG° increase of 1.1 ± 0.2 kcal·mol^{-1}). Surprisingly, this was due to a drastic enthalpy penalty (3.7 ± 0.6 kcal·mol^{-1}) partly compensated by a favorable entropy ($\Delta(-T\Delta S^\circ)$ = −2.6 ± 0.7 kcal·mol^{-1}).

DISCUSSION

ITC: Global Modeling of Direct and Reverse Titrations. ITC is a powerful and reliable method for accurate

DOI: 10.1021/acs.biochem.5b00722
Biochemistry 2015, 54, 5147−5156

determination of thermodynamic parameters, but the origin of errors, and specifically the molecular concentrations, has to be carefully considered to avoid misinterpretation of results. Indeed, K_a and $\Delta H°$ are directly proportional to the concentration $[X_0]$ of the titrant, and the stoichiometry parameter n is proportional to $[X_0]/[M_0]$, where $[M_0]$ is the titrated molecule concentration. Consequently, in the usual analysis, the refined n parameter, which is determined from the half saturation point of the thermogram, serves to correct the stated concentrations and errors volumes.[32] Another consequence of this dependence is that $\Delta G°$ may be measured with a greater accuracy than $\Delta H°$, because $\Delta G° = -RT \ln K_a$. In the current titrations, for a single titration with $\Delta H° = -16.0$ kcal·mol^{-1} and $\Delta G°$ in the range -6.3 to -10.1 kcal·mol^{-1}, an estimated 5% error on titrant concentration $[X_0]$ leads to errors on $\Delta G°$, $\Delta H°$, and $T\Delta S°$ values of respectively 0.03 kcal·mol^{-1}, 0.80 kcal·mol^{-1}, and 0.83 kcal·mol^{-1}. In the literature, analytical estimations of experimental errors with thermodynamic parameters in the same order of magnitude give approximately 0.1−0.4 kcal·mol^{-1}, 0.3−0.7 kcal·mol^{-1}, and 0.3−0.7 kcal·mol^{-1} on $\Delta G°$, $\Delta H°$, and $T\Delta S°$, respectively.[33−35] Most notably the strong correlation between $\Delta H°$ and $T\Delta S°$ measurements in ITC may induce misleading interpretation of small variations.[36] For this set of measurements, the use of global modeling of 2−6 thermograms for each peptide reduces significantly errors in $\Delta G°$, $\Delta H°$, and $T\Delta S°$ values which reach on average respectively 0.10, 0.45, and 0.55 kcal·mol^{-1}. However, we focused our data interpretation mainly on $\Delta\Delta G°$ values and on large enthalpy or entropy variations.

The ITC results presented here constitute one of the first extensive studies of K_d determination for this series of VEGF binding peptides.[10] They allow the comparison of the relative contributions of $\Delta H°$ and $\Delta S°$ to the binding constant for v114* and for the newly synthesized peptide analogues.

The results we obtained for the v114* peptide with two-site inhibitor competition on VEGF ($K_d = 1/K_1 = 28 \pm 7$ nM) are equivalent to those obtained previously by fluorescence polarization using a model of one site inhibitor competition in which $K_i = 60$ nM.[12] As noticed for the parent peptide v107, the binding energy is mainly driven by enthalpy for all of the peptides, whereas the entropy contribution is unfavorable.[10] That is the opposite for natural ligands whose binding energies are dominated by favorable entropy contribution, as shown in VEGF-B/VEGFR1, PlGF/VEGFR1, and VEGF-A/VEGFR2 interactions.[37,38] This peptide property leads to a decrease in K_d as temperature increases (Table 3). Therefore, future improvement of peptides could be achieved by reducing $-T\Delta S°$.

Comparison of Competition Assay and ITC. The correlation between our biochemical model and the experimental data seems significant, indicating that the displacement assay is useful for an approximate affinity ranking of the compounds (Figure 3, Table 3). When compared to K_d, the K_i values extrapolated from IC_{50} using eq 9 are of the same order of magnitude, with the average value of $K_i/K_d = 2.0$ (Std = 1.7) (Figure 3). However, we observe a high nonspecific binding ($\varepsilon = 2.1$ μM) with regard to the K_d values. Consequently the use of this empirical linear equation is restricted to series of compounds with similar nonspecific binding. Moreover the K_i extrapolations are significant for IC_{50} values higher than ε. It results in a less accurate distinction among the higher affinity ligands. Importantly, peptide **12** is an outsider, whose behavior cannot be explained by nonspecific binding, and misleading information may be deduced from the displacement assay. This error may arise from the presence of small quantities of impurities in the sample, even though HPLC and MALDI analysis are satisfactory (>99%) after semipreparative HPLC purification. Indeed, because the final concentration of *bt*VEGF is 20 pM, even 0.1% impurity in samples at 10 μM would still be 500-fold more concentrated than the protein in solution. This is not true for ITC experiments, in which ligand and protein are present at similar concentrations. Therefore, the study presented herein represents an insightful example of a comprehensive comparison between a displacement assay method and an accurate K_d determination method. Displacement assays have a higher throughput, use less protein and ligand, and are better suited for the screening of large libraries of compounds. However, the occurrence of false positive observed here for a very well-defined library of peptides of high purity suggests that ITC may be better suited for this type of SAR study.[33] Consequently, screening of libraries of compounds of lower purities (<98%) by such displacement assays should be carefully controlled.

Effects of Chemical Modification. A series of 17 analogues of the parent peptide have been produced and evaluated by displacement assays and ITC. Several conclusions can be drawn from this study.

We have shown that N-terminal deletion of four amino acids induces a moderate loss of affinity as was expected from alanine scan and fluorescence polarization studies.[9,11,12] Moreover, the four amino acid replacements by different hydrocarbon substituents and the N-terminal deamination have only a slight effect on peptide affinity with VEGF. In the v107-VEGF NMR structure, the N-terminal moiety of the peptide does not interact with the growth factor.[9] However, it is packed on a α-helical segment of the peptide, which may constrain the structure. All together, these results show that N-terminal modifications of the parent peptide are well tolerated and indicate that a variety of functional groups could be introduced for future labeling studies. Our results show also that the loss of affinity may be essentially restored by N-terminal acetylation of Cys 5.

The C-terminal Leu 19 caps the α-helical segment in the NMR structure. Here we show that its deletion induces a 5-fold loss of affinity in two different peptides (**7** and **10**), and small differences observed in CD spectra suggest that the Leu 19 deletion reduces the peptides' structuration (Figure 4). This may be the consequence of α-helix destabilization, or the loss of van der Waals interactions of Leu 19 with the VEGF residues Met 81, Lys 48, and Ile 83, which are observed in the v107-VEGF NMR structure.[9]

In addition, a large dependence of the affinity on cycle size has been demonstrated. Because the disulfide bridge is exposed to the solvent and not directly in contact with the VEGF, we assumed that the loss in affinity was primarily a consequence of an increased flexibility of the peptides. Indeed, increasing the size of the macrocycle could result in unfavorable entropy. However, the CD results are almost identical (peptides **7**−**11**, Figure 4), and no significant entropy changes are observed. Consequently, when adding one or two methylene groups to increase the cycle size, the subtle changes in the conformation impact peptide−protein or peptide-solvent interactions and induce a loss of affinity which is mainly enthalpy-driven. Replacement of the disulfide by a thioether bridge decreases the affinity. However, it has to be pointed out that the peptide **14** is present as a mixture of diastereomers. Consequently it is

DOI: 10.1021/acs.biochem.5b00722
Biochemistry 2015, 54, 5147−5156

premature to decipher the specific effects of this chemical modification.

The behavior of peptide **17**, in which the Phe 16 is substituted by a fluorine atom, is particularly interesting. It displays an especially low, albeit positive, entropy contribution to binding, as compared to the other peptides ($\Delta(-T\Delta S°)$ = 1.0−4.2 kcal·mol^{-1}). Phe 16 is the most buried residue at the interface with VEGF, and alanine mutation results in a drastic loss of affinity.[9] One hypothesis is the modification of the hydration shell and of different interactions with the VEGF, which may be drastically affected. Indeed, recent results in the literature indicate that the fluorination of human carbonic anhydrase binding ligands and the halogenation of ligands of the third PDZ domain of a mammalian neuronal protein both lead to similar entropy gains, compensated by enthalpy losses. In these cases, an explanation based on the hydrophobic effect and reorganization of water molecules upon binding has been suggested.[35,39]

We have proposed above that future improvement of peptides could be achieved by reducing the entropy penalty of binding to VEGF. Two paths are opened by this study: the first one will be to reduce the conformational freedom by the introduction of chemical constraints, and the second one will be to explore alternative fluorination patterns of Phe 16.

■ ASSOCIATED CONTENT

Supporting Information

The Supporting Information is available free of charge on the ACS Publications website at DOI: 10.1021/acs.biochem.5b00722.

Supplemental tables and figures (PDF)

■ AUTHOR INFORMATION

Corresponding Authors

*(J.-F.G.) E-mail: jean-francois.gaucher@parisdescartes.fr. Phone: (33) 170649407. Fax: (33) 153739925.

*(S.B.) E-mail: sylvain.broussy@parisdescartes.fr. Phone: (33) 153731564. Fax: (33) 143291403.

Funding

Financial support from the French National Research Agency (ANR-2010-BLAN-1533-03), the University Paris Descartes, the CNRS ("Chaire de Partenariat CNRS" to S.B.), and the ARC (Grant DOC2013 0606849 to M.R.-S.) is acknowledged.

Notes

The authors declare no competing financial interest.

■ ACKNOWLEDGMENTS

We thank Dr. S. Bouaziz (Paris-Descartes University, France) for the use of a CD instrument, Dr. D. Scherman (Paris-Descartes University, France) for the use of a chemiluminescence plate reader, and Dr. S. Coulthurst for careful rereading of the manuscript (University of Dundee, Scotland).

■ REFERENCES

(1) Hanahan, D., and Weinberg, R. A. (2011) Hallmarks of cancer: the next generation. *Cell 144*, 646−674.

(2) Carmeliet, P., and Jain, R. K. (2000) Angiogenesis in cancer and other diseases. *Nature 407*, 249−257.

(3) Carmeliet, P., and Jain, R. K. (2011) Molecular mechanisms and clinical applications of angiogenesis. *Nature 473*, 298−307.

(4) Ferrara, N. (2009) Vascular Endothelial Growth Factor. *Arterioscler., Thromb., Vasc. Biol. 29*, 789−791.

(5) Williams, D. F., et al. (2011) Ranibizumab and Bevacizumab for Neovascular Age-Related Macular Degeneration. *N. Engl. J. Med. 364*, 1897−1908.

(6) Fedorova, A., Zobel, K., Gill, H. S., Ogasawara, A., Flores, J. E., Tinianow, J. N., Vanderbilt, A. N., Wu, P., Meng, Y. G., Williams, S.-P., Wiesmann, C., Murray, J., Marik, J., and Deshayes, K. (2011) The Development of Peptide-Based Tools for the Analysis of Angiogenesis. *Chem. Biol. 18*, 839−845.

(7) Fairbrother, W. J., Christinger, H. W., Cochran, A. G., Fuh, G., Keenan, C. J., Quan, C., Shriver, S. K., Tom, J. Y. K., Wells, J. A., and Cunningham, B. C. (1998) Novel peptides selected to bind vascular endothelial growth factor target the receptor-binding site. *Biochemistry 37*, 17754−17764.

(8) Kenrick, S. A., and Daugherty, P. S. (2010) Bacterial display enables efficient and quantitative peptide affinity maturation. *Protein Eng., Des. Sel. 23*, 9−17.

(9) Pan, B., Li, B., Russell, S. J., Tom, J. Y. K., Cochran, A. G., and Fairbrother, W. J. (2002) Solution structure of a phage-derived peptide antagonist in complex with vascular endothelial growth factor. *J. Mol. Biol. 316*, 769−787.

(10) Dyachenko, A., Goldflam, M., Vilaseca, M., and Giralt, E. (2010) Molecular Recognition at Protein Surface in Solution and Gas Phase: Five VEGF Peptidic Ligands Show Inverse Affinity When Studied by NMR and CID-MS. *Biopolymers 94*, 689−700.

(11) Peterson, K. J., Sadowsky, J. D., Scheef, E. A., Pal, S., Kourentzi, K. D., Willson, R. C., Bresnick, E. H., Sheibani, N., and Gellman, S. H. (2008) A fluorescence polarization assay for identifying ligands that bind to vascular endothelial growth factor. *Anal. Biochem. 378*, 8−14.

(12) Haase, H. S., Peterson-Kaufman, K. J., Lan Levengood, S. K., Checco, J. W., Murphy, W. L., and Gellman, S. H. (2012) Extending foldamer design beyond α-helix mimicry: α/β-peptide inhibitors of Vascular Endothelial Growth Factor signaling. *J. Am. Chem. Soc. 134*, 7652−7655.

(13) Gautier, B., Goncalves, V., Diana, D., Di Stasi, R., Teillet, F., Lenoir, C., Huguenot, F., Garbay, C., Fattorusso, R., D'Andrea, L. D., Vidal, M., and Inguimbert, N. (2010) Biochemical and structural analysis of the binding determinants of a vascular endothelial growth factor receptor peptidic antagonist. *J. Med. Chem. 53*, 4428−4440.

(14) Gautier, B., Miteva, M. A., Goncalves, V., Huguenot, F., Coric, P., Bouaziz, S., Seijo, B., Gaucher, J.-F., Broutin, I., Garbay, C., Lesnard, A., Rault, S., Inguimbert, N., Villoutreix, B. O., and Vidal, M. (2011) Targeting the proangiogenic VEGF-VEGFR protein-protein interface with drug-like compounds by in silico and in vitro screening. *Chem. Biol. 18*, 1631−1639.

(15) Goncalves, V., Gautier, B., Garbay, C., Vidal, M., and Inguimbert, N. (2007) Development of a chemiluminescent screening assay for detection of vascular endothelial growth factor receptor 1 ligands. *Anal. Biochem. 366*, 108−110.

(16) Pace, C. N., Vajdos, F., Fee, L., Grimsley, G., and Gray, T. (1995) How to measure and predict the molar absorption coefficient of a protein. *Protein Sci. 4*, 2411−2423.

(17) Ellman, G. L. (1959) Tissue sulfhydryl groups. *Arch. Biochem. Biophys. 82*, 70−77.

(18) Riddles, P. W., Blakeley, R. L., and Zerner, B. (1979) Ellman's reagent: 5,5′-dithiobis(2-nitrobenzoic acid) - a reexamination. *Anal. Biochem. 94*, 75−81.

(19) Christinger, H. W., Muller, Y. A., Berleau, L. T., Keyt, B. A., Cunningham, B. C., Ferrara, N., and de Vos, A. M. (1996) Crystallization of the receptor binding domain of vascular endothelial growth factor. *Proteins: Struct., Funct., Genet. 26*, 353−357.

(20) Zhao, H., and Schuck, P. (2015) Combining biophysical methods for the analysis of protein complex stoichiometry and affinity in SEDPHAT. *Acta Crystallogr., Sect. D: Biol. Crystallogr. 71*, 3−14.

(21) Zhao, H., Piszczek, G., and Schuck, P. (2015) SEDPHAT - A platform for global ITC analysis and global multi-method analysis of molecular interactions. *Methods 76*, 137−148.

(22) Houtman, J. C. D., Brown, P. H., Bowden, B., Yamaguchi, H., Appella, E., Samelson, L. E., and Schuck, P. (2007) Studying multisite binary and ternary protein interactions by global analysis of isothermal

DOI: 10.1021/acs.biochem.5b00722
Biochemistry 2015, 54, 5147−5156

titration calorimetry data in SEDPHAT: Application to adaptor protein complexes in cell signaling. *Protein Sci. 16*, 30−42.
(23) Subirós-Funosas, R., Prohens, R., Barbas, R., El-Faham, A., and Albericio, F. (2009) Oxyma: An Efficient Additive for Peptide Synthesis to Replace the Benzotriazole-Based HOBt and HOAt with a Lower Risk of Explosion. *Chem. - Eur. J. 15*, 9394−9403.
(24) Cochran, A. G., Skelton, N. J., and Starovasnik, M. A. (2001) Tryptophan zippers: Stable, monomeric β-hairpins. *Proc. Natl. Acad. Sci. U. S. A. 98*, 5578−5583.
(25) Wu, L., McElheny, D., Huang, R., and Keiderling, T. A. (2009) Role of Tryptophan-Tryptophan Interactions in Trpzip β-Hairpin Formation, Structure, and Stability. *Biochemistry 48*, 10362−10371.
(26) Mayer, J. P., Zhang, J., Groeger, S., Liu, C.-F., and Jarosinski, M. A. (1998) Lanthionine macrocyclization by in situ activation of serine. *J. Pept. Res. 51*, 432.
(27) Yu, L., Lai, Y., Wade, J. W., and Coutts, S. M. (1998) A Simple and Efficient Method for the Syntheses of Thioether Cyclic Peptides. *Tetrahedron Lett. 39*, 6633−6636.
(28) Harpp, D. N., and Gleason, J. G. (1971) Organic Sulfur Chemistry. X. Selective Desulfurization of Disulfides. Scope and Mechanism. *J. Am. Chem. Soc. 93*, 2437−2445.
(29) Harpp, D. N., and Gleason, J. G. (1971) Preparation and Mass Spectral Properties of Cystine and Lanthionine Derivatives. A Novel Synthesis of L-Lanthionine by Selective Desulfurization. *J. Org. Chem. 36*, 73−80.
(30) Galande, A. K., Trent, J. O., and Spatola, A. F. (2003) Understanding Base-Assisted Desulfurization Using a Variety of Disulfide-Bridged Peptides. *Biopolymers 71*, 534−551.
(31) Cheng, Y.-C., and Prusoff, W. H. (1973) Relationship between the inhibition constant (K_i) and the concentration of inhibitor which causes 50% inhibition (I_{50}) of an enzymatic reaction. *Biochem. Pharmacol. 22*, 3099−3108.
(32) Tellinghuisen, J., and Chodera, J. D. (2011) Systematic errors in isothermal titration calorimetry: concentrations and baselines. *Anal. Biochem. 414*, 297−299.
(33) Torres, F. E., Recht, M. I., Coyle, J. E., Bruce, R. H., and Williams, G. (2010) Higher throughput calorimetry: opportunities, approaches and challenges. *Curr. Opin. Struct. Biol. 20*, 598−605.
(34) Krishnamurthy, V. M., Bohall, B. R., Semetey, V., and Whitesides, G. M. (2006) The Paradoxical Thermodynamic Basis for the Interaction of Ethylene Glycol, Glycine, and Sarcosine Chains with Bovine Carbonic Anhydrase II: An Unexpected Manifestation of Enthalpy/Entropy Compensation. *J. Am. Chem. Soc. 128*, 5802−5812.
(35) Breiten, B., Lockett, M. R., Sherman, W., Fujita, S., Al-Sayah, M., Lange, H., Bowers, C. M., Heroux, A., Krilov, G., and Whitesides, G. M. (2013) Water Networks Contribute to Enthalpy/Entropy Compensation in Protein−Ligand Binding. *J. Am. Chem. Soc. 135*, 15579−15584.
(36) Chodera, J. D., and Mobley, D. L. (2013) Entropy-enthalpy compensation: role and ramifications in biomolecular ligand recognition and design. *Annu. Rev. Biophys. 42*, 121−142.
(37) Leppänen, V.-M., Prota, A. E., Jeltsch, M., Anisimov, A., Kalkkinen, N., Strandin, T., Lankinen, H., Goldman, A., Ballmer-Hofer, K., and Alitalo, K. (2010) Structural determinants of growth factor binding and specificity by VEGF receptor 2. *Proc. Natl. Acad. Sci. U. S. A. 107*, 2425−2430.
(38) Anisimov, A., Leppänen, V.-M., Tvorogov, D., Zarkada, G., Jeltsch, M., Holopainen, T., Kaijalainen, S., and Alitalo, K. (2013) The Basis for the Distinct Biological Activities of Vascular Endothelial Growth Factor Receptor-1 Ligands. *Sci. Signaling 6*, ra52.
(39) Memic, A., and Spaller, M. R. (2008) How Do Halogen Substituents Contribute to Protein-Binding Interactions? A Thermodynamic Study of Peptide Ligands with Diverse Aryl Halides. *ChemBioChem 9*, 2793−2795.

DOI: 10.1021/acs.biochem.5b00722
Biochemistry 2015, 54, 5147−5156